Dynamic Interaction between Paramagnetic Ions and Resonant Phonons in a Bottlenecked Lattice*

WILLIAM J. BRYA† AND PETER E. WAGNER‡
Department of Electrical Engineering and Carlyle Barton Laboratory, The Johns Hopkins University, Baltimore, Maryland

(Received 20 October 1966)

Anomalous behavior is observed in the time dependence of paramagnetic relaxation for dilute cerous magnesium nitrate at Zeeman frequencies of 11 GHz, temperatures 1.2–4.2°K, and nominal cerium concentrations of 0.2%. Immediately after excitation of the paramagnetic transition to a negative spin temperature, direct relaxation is accompanied by heating of the resonant lattice modes, and a "phonon avalanche" occurs. The decay profile of the center of the paramagnetic resonance line is distorted in a characteristic manner, and certain peculiarities in the shape of the line appear. Later in the decay, after the spin temperature has become positive, the decay approaches the behavior customarily identified with a phonon bottleneck, and the line shape becomes normal. The avalanche builds up on a time scale of microseconds, while the decay at positive spin temperature requires tens of milliseconds. Concentration, size, and surface effects are found. A simple theoretical model is developed and shown to agree qualitatively, but not quantitatively, with experiment.

I. INTRODUCTION

IT is well known that the paramagnetic heat capacity of an ensemble of impurity ions in a crystal can be greater by many orders of magnitude than that of the lattice vibrations to which the ions are coupled. Energy that is stored in magnetic form and then transferred selectively into a narrow band of lattice modes may therefore cause considerable heating of these modes. A necessary condition is that the resonant ion-phonon interaction be strong and the coupling of the heated modes to the thermal environment be comparatively weak. This situation is termed a phonon bottleneck[1]; it is especially likely to occur in the relaxation of an excited paramagnetic transition at low temperatures, for cases in which the direct relaxation rate is large, the indirect rates are weak, and the phonon lifetime (apart from interaction with the ions) is long.

The techniques of paramagnetic resonance are well suited to a study of the bottleneck. They involve the electromagnetic excitation of a paramagnetic transition and the subsequent observation of energy which has been transferred into resonant lattice modes by the mechanism of direct paramagnetic relaxation. Lattice excitation, however, is not detected directly, but by its back reaction on the paramagnetic transition. In one such experiment, Faughnan and Strandberg[2] attempted without success to first generate hot phonons by continuous microwave saturation of spins at one end of a crystal and then detect the phonons by reabsorption in spins at the other end.

More fruitful results have been obtained in studies of the dynamics of relaxation. If the populations of the levels making up a paramagnetic transition are suddenly disturbed, and if there is no bottleneck, the subsequent decay of the magnetization is expected to vary exponentially in time. If, however, a bottleneck is present, the resonant phonons generated during the decay cannot be dissipated, and they distort the decay profile. Giordmaine *et al.*[3] attempted to measure the time decay for several salts, with results that were not susceptible to straightforward interpretation. Excitation was accomplished by the application of saturating pulses; some attempts were also made to invert the magnetization by adiabatic fast passage. More recently, a number of authors have observed bottleneck effects by studying the dependence on size and paramagnetic concentration of the relaxation profiles following microwave saturating pulses.[4–6] These parameters should affect the magnitude of the bottleneck because they influence the rate at which phonons interact with spins relative to the rate at which phonons escape to the thermal bath.

Of the various microwave methods, measurement of the transient decay of an inverted paramagnetic transition is by far the most sensitive, because it represents the interaction of a system initially at negative temperature with one whose temperature must always be positive. Consider the case of an isolated Kramers doublet, taken to be the ground state of a paramagnetic ion in a nonmagnetic host crystal. A Zeeman field splits the doublet by an energy δ, with populations n_1 and n_2 in the lower and upper states, respectively; the initial condition is $n_2 > n_1$. At low temperature, where only the direct process is active, the populations then

* This research was supported by the Air Force Avionics Laboratory, Research and Technology Division, Air Force Systems Command, U. S. Air Force under Contract No. AF 33(615)-3585.

† Present address: Bell Telephone Laboratories, Murray Hill, New Jersey.

‡ On leave. Present address: Clarendon Laboratory, Oxford University, Oxford, England.

[1] J. H. Van Vleck, Phys. Rev. **59**, 724 (1941).

[2] B. W. Faughnan and M. W. P. Strandberg, J. Phys. Chem. Solids **19**, 155 (1961).

[3] J. A. Giordmaine, L. E. Alsop, F. R. Nash, and C. H. Townes, Phys. Rev. **109**, 302 (1958).

[4] P. L. Scott and C. D. Jeffries, Phys. Rev. **127**, 32 (1962); R. H. Ruby, H. Benoit, and C. D. Jeffries, Phys. Rev. **127**, 51 (1962).

[5] F. R. Nash, Phys. Rev. **138**, A1500 (1965).

[6] K. J. Standley and J. K. Wright, Proc. Phys. Soc. (London) **83**, 361 (1964).

decay toward their thermal equilibrium values by means of the absorption and emission of resonant lattice quanta. The instantaneous logarithmic decay rate is proportional to $2p+1$, where p is the excitation number of the resonant lattice modes. If, on one hand, the phonons generated during the decay are immediately absorbed by the thermal bath, p always remains fixed at its equilibrium value, and an exponential decay profile is observed. On the other hand, if the phonons cannot be absorbed, the value of p, and thus the instantaneous decay rate, must increase and accelerate the emission of still more quanta in a regenerative manner. The net result is a kind of phonon avalanche and a sudden reduction in the magnitude of the inverted spin resonance line. Eventually the ions and phonons attain a common (positive) temperature and the avalanche stops, after which the joint system relaxes toward thermal equilibrium over a much longer interval.

Thus, after inversion, the bottleneck is manifested by a delayed, sudden decay of the inverted line, followed by a sharp knee and a slow recovery to thermal equilibrium. The decay is all important because it implies regeneration and therefore rules out alternative mechanisms (for example, cross relaxation to other magnetic impurities). By way of contrast, a saturating pulse does not excite an avalanche, because the spin temperature is never negative. The time decay is still nonexponential, but does not display the delayed step which is so uniquely characteristic of the bottleneck. In practice, pulse saturation-recovery experiments have proved useful only for studying the decay curves at late times, near thermal equilibrium.

Early measurements of the phonon avalanche in dilute cerous magnesium nitrate were reported recently.[7,8] Similar behavior has been found in dilute potassium ferricyanide[9] and nickel- and iron-doped MgO.[10] In the present paper we describe the experimental behavior of the cerium salt in greater detail. Section II contains a theoretical analysis based on an extension of the approach of Faughnan and Strandberg.[2] The microwave apparatus and techniques of measurement are described in III, and IV is concerned with a description of the paramagnetic material. Experimental results are presented and interpreted in V, and our conclusions are summarized in VI. The Appendix is concerned with an incidental effect which can distort observed decay profiles in certain circumstances.

II. THEORY

The simplest model is based on rate equations for the level populations n_1, n_2 and the phonon excitation p. A linear loss mechanism for the phonons is assumed, such that the lifetime T_p would be constant in the absence of interaction with the ions. It should be recognized at the outset that this model suffers several defects: The actual loss mechanism for phonons undoubtedly involves their destruction at the surface of the crystal; hence T_p, and therefore n_1, n_2, and p, all depend on spatial position inside the sample. This dependence is disregarded. In addition, the fact that the propagation medium for phonons is anisotropic and that there are three acoustical modes, all of which may behave differently, is neglected. Finally, since the avalanche is regenerative, some coherence may be present in the phonons, which again is disregarded. The model is nevertheless useful because it is tractable, it shows avalanche behavior, it agrees in some aspects with experiment, and it provides a simple physical framework for understanding the dynamics of the process.

The rate equations can be written,

$$d(n_2-n_1)/dt=-2A[(p+1)n_2-pn_1] -[(n_2-n_1)+(n_1^0-n_2^0)]T_{1I}^{-1},$$

where A is the spontaneous emission rate for direct relaxation, T_{1I}^{-1} is the relaxation rate for all indirect processes, and the superscript denotes thermal equilibrium. For the phonons, we write[2]

$$dp/dt=-[2\rho(\delta)d\delta]^{-1}d(n_2-n_1)/dt-(p-p^0)T_p^{-1},$$

where $\rho(\delta)d\delta$ is the number of lattice states which interact with the ions, and δ is the energy of the transition. Let

$$u=(n_2-n_1)/(n_1^0-n_2^0), \qquad y=(p-p^0)/(p^0+\tfrac{1}{2}).$$

These variables represent normalized values for the population difference and the deviation of the phonon excitation from equilibrium. After some rearrangement, the rate equations become,

$$du/dt = -(u+1)T_{1D}^{-1}-uyT_{1D}^{-1}-(u+1)T_{1I}^{-1}, \quad (1a)$$

$$dy/dt = -yT_p^{-1}+S(u+1)T_{1D}^{-1}+SuyT_{1D}^{-1} \quad (1b)$$

$$= [-y+\sigma(u+1)+\sigma uy]T_p^{-1}, \quad (1c)$$

where $S=(n_1^0-n_2^0)/(2p^0+1)\rho(\delta)d\delta$ is the ratio of the thermal equilibrium energy stored in the paramagnetic transition to that stored in the resonant lattice modes, $\sigma=ST_p/T_{1D}$ is the "bottleneck factor," and $T_{1D}^{-1}=A(2p^0+1)$ is the direct relaxation rate at the ambient temperature. In Eq. (1a) the first and last terms represent ordinary direct and indirect relaxation, and the center term gives the component of the decay rate due to excess phonons. This term [and its counterpart in Eq. (1b)] is responsible for the avalanche. In our experiments, y is always positive, so this term always tends to damp the population difference asymptotically to infinite spin temperature.

[7] W. J. Brya and P. E. Wagner, Phys. Rev. Letters **14**, 431 (1965).
[8] P. E. Wagner and W. J. Brya, *Physics of Quantum Electronics* (McGraw-Hill Book Company, Inc., New York, 1966), p. 376.
[9] R. F. David and P. E. Wagner, Phys. Rev. **150**, 192 (1966).
[10] N. S. Shiren (private communication).

The bottleneck parameter σ represents the ratio of power transferred from ions to phonons to power transferred from phonons to thermal bath. Thus, if $\sigma \ll 1$, Eqs. (1) should yield normal relaxation; however, if $\sigma \gg 1$, the time decay should show behavior characteristic of a severe bottleneck. At liquid-helium temperatures and microwave frequencies the phonon lifetime is expected to be determined by processes at the surfaces of the crystal. For a flat platelet, T_p is presumably proportional to the time of flight of a phonon across the crystal; hence, σ should be proportional to the thickness. (This dependence may, however, be altered if the surface does not correspond to an acoustically matched boundary.) Also, if T_p and $d\delta$ are independent of frequency and temperature, and if the density of states obeys the Debye law, then, for a Kramers transition, $\sigma \propto (\delta^3/d\delta) \tanh(\delta/2kT) \propto \delta^4/Td\delta$ for small δ/kT. The bottleneck should therefore disappear at low Zeeman frequencies, as has been observed.[11]

Because the rate equations are not linear, they do not appear to be soluble except by numerical techniques; however, the solutions for certain special cases are very useful and revealing. Note first that immediately after a perturbation has been applied to the spin system only, so that the phonon excitation is zero, the resonance line begins to decay with the normal rate, $T_{1D}^{-1}+T_{1I}^{-1}$. Later, at $u=0$ (saturation of the resonance line), the logarithmic slope is again $T_{1D}^{-1}+T_{1I}^{-1}$, independent of the strength of the bottleneck. This fact is a consequence of the cancellation of induced emission and absorption: Only the spontaneous emission of resonant lattice quanta remains, irrespective of the amount of lattice excitation. The indirect processes, of course, are unaffected by the number of phonons at δ. This feature allows a determination of the normal relaxation rates in the presence of a bottleneck by a measurement of the instantaneous decay slope at saturation.[12] Such measurements are reported elsewhere.[11]

The behavior of u and y can also be determined easily near the end of the decay, where $u \to -1$ and $y \to 0$. The rate equations can be linearized to yield

$$d(u+1)/dt = -(T_{1D}^{-1}+T_{1I}^{-1})(u+1)+T_{1D}^{-1}y,$$

$$dy/dt = -(\sigma+1)T_p^{-1}y+\sigma T_p^{-1}(u+1).$$

The solutions contain two decay rates, the slower of which is

$$T_{1A}^{-1}=[(\sigma+1)T_{1D}]^{-1}+T_{1I}^{-1}.$$

The quantity T_{1A} is the asymptotic time constant obtained in previous pulse-saturation studies.[4-6] Since $\sigma \propto T^{-1}$ and $T_{1D}^{-1} \propto T$, the asymptotic direct rate becomes

$$T_{1A}^{-1}=(1/DT^2+1/BT)^{-1}+T_{1I}^{-1}$$

$$=BDT^2/(B+DT)+T_{1I}^{-1}, \quad (2)$$

where B and D are constants. Thus, as one proceeds from a condition of no bottleneck to one of a severe bottleneck, the temperature variation of the apparent direct rate should change from T to T^2. Also, this rate should depend on crystal size and surface (through T_p), on concentration (through S), and on frequency.

The behavior of the spin resonance line at short times, when $u>0$, is by far the most interesting. Figure 1 shows some solutions to the rate equations which were generated on an IBM 7094 computer. The values used for these curves are typical of experimental conditions for the cerium salt. The quantity $S=2.5\times10^4$ was estimated by taking a density of paramagnetic ions of $3\times10^{18}/\text{cm}^3$, a temperature of 1.4°K, a sound velocity $\sim2.5\times10^5$ cm/sec, a frequency of 11 GHz, and a bandwidth approximately equal to the resonance linewidth, 15 MHz. The phonon lifetime $T_p=1$ μsec was taken to be equal to the transit time through a typical sample, for reasons which are discussed below.

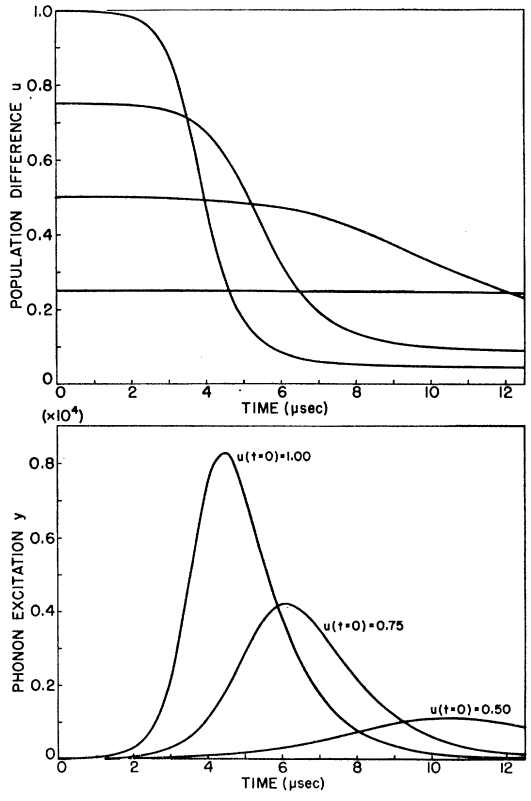

FIG. 1. Solutions to Eqs. (1) for negative spin temperature and for $S=2.5\times10^4$, $T_p=1$ μsec, $T_{1D}=10$ msec, $T_{1I}\to\infty$.

[11] W. J. Brya and P. E. Wagner, Phys. Rev. **147**, 239 (1966).

[12] This measurement, however, presupposes that the decay at saturation is governed only by paramagnetic relaxation and not by, e.g., spin diffusion. Thus, the initial decay slope after excitation by a saturating pulse would be suspect; there is no guarantee that the pulse generates infinite spin temperature through the entire resonance line.

Solutions are shown for several initial values of u, but in all cases $y=0$ at $t=0$ is assumed. The most dramatic features of the decay of u are the delayed step and the slowing down prior to saturation. The initial value of u has a pronounced effect on the decay: the step is delayed longer and is less abrupt for smaller initial degrees of inversion.

The behavior of y is also shown. The phonon excitation increases to a maximum and then returns to equilibrium as the excess phonon energy is dissipated. The quantity y closely approximates the ratio of the temperature of the resonant phonons to the bath temperature. For example, for $u(t=0)=1$, the phonon excitation reaches a value 8×10^8, corresponding to a phonon temperature of 11×10^3°K at a bath temperature of only 1.4°K. This fact illustrates the inadequacy of the resonant phonons to act as a reservoir, even when the destruction of phonons is relatively efficient.

For a given initial value of u, the behavior of the fast decay under variations of S and T_p is shown in Fig. 2. As one might expect, the decay step is sharper and occurs earlier for large S and T_p; however, it is not possible to compensate exactly for a change in one parameter by adjustment of the other one.

The effect of nonzero initial values of y was also examined, but is not shown. In general, the shape of the decay is altered only slightly, but the decay curves appear to be translated in time; that is, a curve for $y(t=0)>0$ can be superimposed on the curve for $y(t=0)=0$ by a simple time shift.

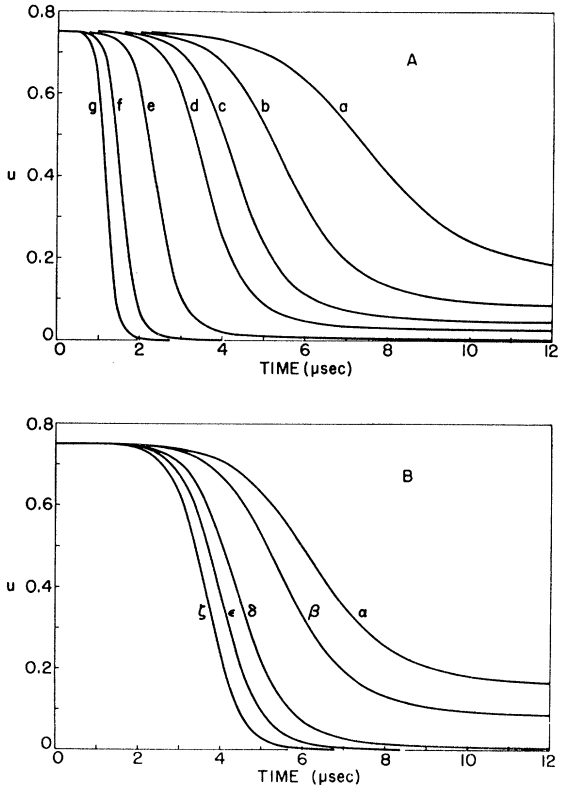

FIG. 2. Solutions to Eqs. (1) for $T_{1D}=10$ msec and $T_{1I}\rightarrow\infty$. A, a through g: $T_p=1$ μsec; $10^{-4}S=2$, 2.5, 3, 3.5, 5, 7.5, and 10, respectively. B, α through ζ: $S=2.5\times10^4$; $T_p=0.8$, 1.0, 2.0, 4.0, and ∞ μsec, respectively.

Equations (1) can be solved exactly in the limit of large σ. The solutions have been given elsewhere[8] and are included here for completeness. For $S\gg1$, they are

$$u=u^i/\{1+\exp[(t-T_{1/2})/T_f]\},$$

$$y=Su^i/\{1+\exp[-(t-T_{1/2})/T_f]\},$$

where

$$T_f^{-1}=Su^iT_{1D}^{-1}=A(n_2^i-n_1^i)/\rho(\delta)\,d\delta,$$

and

$$T_{1/2}=T_f\ln[S(u^i)^2/(u^i+1)].$$

The superscript denotes the initial value.

In summary, the rate equations predict three different modes of decay, corresponding to the cases $u>0$, $u=0$, and $u\rightarrow-1$. Direct relaxation has a characteristic time in each case. For negative spin temperature, this time is T_f, which can be recognized as the re-emission time for a phonon in the presence of $n_2^i-n_1^i$ spins. At infinite spin temperature, the characteristic time is just T_{1D}, and near thermal equilibrium it is roughly $T_{1A}=(\sigma+1)T_{1D}$. For a strong effect, $T_f\ll T_{1D}\ll T_{1A}$.

In this analysis, any dependence of the decay on spatial inhomogeneities has been neglected. Giordmaine and Nash[13] have considered in detail the spatial effects for values of u and y corresponding to small deviations from thermal equilibrium, and their results will be useful below. For an inhomogeneously broadened resonance line, phonons escape by diffusion through the paramagnetic ions, and the asymptotic time constant T_{1A} found for an infinite slab of thickness L is identical to our expression, providing T_p is taken to be the time of flight of a phonon across the slab. For a homogeneously broadened line, the approach developed by Holstein[14] is applicable. With this model, phonons in interaction with the center of the spin resonance line are dissipated very slowly, but those with frequencies in the relatively transparent wings of the line are thermalized more rapidly. The validity of the model depends on how quickly energy can be distributed throughout the resonance line by the homogenizing mechanism. The time constant T_{1A} is found to be proportional to $NLT^{-2}(d\nu)^{-1}$ for Gaussian line shapes and $(NLT_{1D})^{1/2}(d\nu)^{-1/2}T^{-1}$ for Lorentzian lines, where N is the concentration of ions, L is the thickness of the slab, and $d\nu$ is the linewidth.

III. APPARATUS AND PROCEDURES

The experimental method used in the present study consists of first inverting the spin resonance line by

[13] J. A. Giordmaine and F. R. Nash, Phys. Rev. **138**, A1510 (1965).

[14] T. Holstein, Phys. Rev. **72**, 1212 (1947).

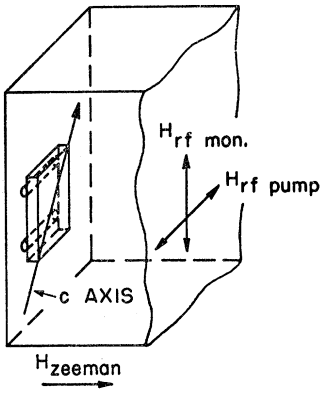

FIG. 3. Section drawing of bimodal cavity, sample, and mounting legs. Microwave magnetic fields for fast passage and monitoring are denoted $H_{\text{rf pump}}$ and $H_{\text{rf mon}}$, respectively.

means of adiabatic fast passage of the magnetic field H through its resonant value, and subsequently observing the time dependence of the whole line (or any portion of it) with a conventional paramagnetic resonance spectrometer. This method is well established[15]; however, the technique as practiced has always been comparatively slow, because of the time variation required for the swept field. In order to induce fast passage and to measure the paramagnetic resonance at the same frequency, dH/dt must necessarily change sign; but with simple circuitry, the sign change consumes a relatively long time. In the present experiment, this problem was circumvented by the use of two Zeeman frequencies, one (ν_p) for fast passage and the other (ν_m) for measurement. Thus the magnetic field could be swept continuously and quickly from the time of passage to the time of measurement. In addition, the high-power microwave pulse required for fast passage at the frequency ν_p could easily be prevented from saturating the receiver, which was tuned to a different microwave frequency ν_m.

Relaxation profiles were measured over the temperature range 1.2–4.2°K. Monitoring power levels typically $\lesssim 10^{-7}$ W were found to be low enough to have no effect on the recovery curves. Superheterodyne detection at ~30 MHz was used, and the intermediate frequency was amplified and rectified with a phase-sensitive second detector. X-13 klystrons served as master and local oscillators. The frequency of the master oscillator was stabilized, but the local oscillator did not require stabilization because only broadband intermediate frequency components were used.

The microwave pulse was obtained from a 50-W pulsed oscillator which utilized a traveling wave amplifier (TWA) with external feedback through a transmission wavemeter, a phase shifter, and a variable attenuator. The oscillator was gated on during passage by a control grid contained in the TWA.

For the reasons discussed above, a bimodal rectangular reflection cavity was employed in the spectrometer. The TE_{102} and TE_{011} modes were used, with frequencies of 11.35 and 11.45 GHz, respectively. The location of the sample, the polarization of the microwave magnetic fields, and the orientation of the Zeeman field are shown in Fig. 3. The cavity was constructed of plastic and silver plated to pass the swept magnetic field, which was obtained from coils attached to the outside of the cavity. The sample was mounted on small Teflon spacers which in turn were attached to the wall of the cavity, in order to permit free circulation of liquid helium about the sample. Silicone vacuum grease was used as an adhesive.

When the sample was inserted, the two modes shifted in frequency by different amounts, and thin Teflon slabs were inserted into the cavity to restore the original mode separation. Variable coupling to each cavity mode was provided by two loop probes which could be adjusted from outside the Dewar.

The temperature of the sample was measured with a calibrated carbon resistor mounted to the outside of the cavity. At low temperatures, electronic temperature control was used; and at higher temperatures, control was accomplished with a vapor pressure regulator which used a thin flexible rubber tube as a variable conductance in the vacuum line from the helium bath.

The time sequences used for gathering data differ from those described in Ref. 7 and are shown in Fig. 4. In the method labeled A, a continuous measurement of the relaxation of the center of the spin resonance line was made. The static magnetic field H_{dc} coincided with the resonant field H_m for frequency ν_m. Fast passage was brought about at field H_p, corresponding to the other cavity mode at frequency ν_p. Inversion was induced on the upsweep, and measurements were possible as soon as the sweep was terminated. Thereafter, the decay of the center of the line was observed continuously and recorded on a storage oscilloscope. A reference trace of the equilibrium signal could be made simply by activating the field sweep but not the pulse. The oscilloscope traces were photographed for later analysis.

The procedure B for observing the entire resonance line during recovery amounted essentially to a simple

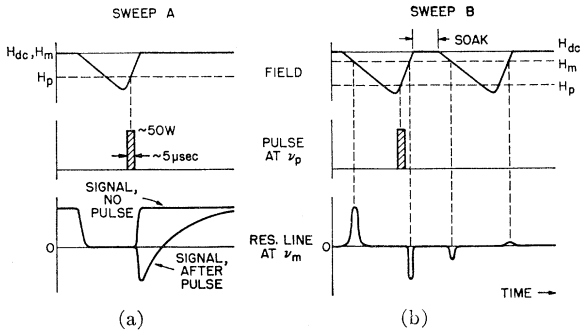

FIG. 4. Time sequences employed for (a) continuous observation of the line center and (b) display of the line shape during recovery. Letters p and m denote passage and monitor, respectively.

[15] A. Rannestad and P. E. Wagner, Phys. Rev. **131**, 1953 (1963).

upward shift of H_{dc}. The line was displayed when the swept field passed through H_m and could be observed once during the initial sweep, and again after a controlled interval (labeled "soak").

There were two sources of incidental distortion in the experiment. First, the change in reflection coefficient was not directly proportional to the population difference u, because the spin resonance was not a negligibly small perturbation on the cavity losses. In the data reduction, all reflection coefficients were therefore converted to effective Q changes.

A second distortion involved a shift of the resonant Zeeman field when the resonance line changed from emission to absorption, that is, when the magnetization changed sign. This effect was important only in more concentrated samples, and it prevented the continuous observation of the line center at early times. It was caused by changes in the demagnetizing field and is discussed in the Appendix.

IV. THE PARAMAGNETIC MATERIAL

Lanthanum magnesium nitrate doped with cerium was used in the experiment. This material was chosen because it was known to display a bottleneck,[4] it is easily grown, and the narrow resonance lines allow a relatively modest magnetic-field sweep. Concentrations of Ce/La=0.2 and 0.5 at.% were studied. These figures refer to the water solution from which the crystals were grown and are not trustworthy; in fact, magnetic measurements indicated wide variations among crystals grown under similar conditions.

At temperatures below 4°K, only the lowest Kramers doublet of Ce^{3+} is populated; and, since there is no hyperfine structure and all the ions are magnetically equivalent, the ion behaves like an ideal spin-$\frac{1}{2}$ system, except for a highly anisotropic g factor.[4] Dipolar broadening is known to be small[16] but becomes important for concentrations $\gtrsim 1\%$. Below this value the broadening is inhomogeneous. The linewidth is anisotropic and has its minimum value of roughly 5 G when the Zeeman field is perpendicular to the crystalline c axis.

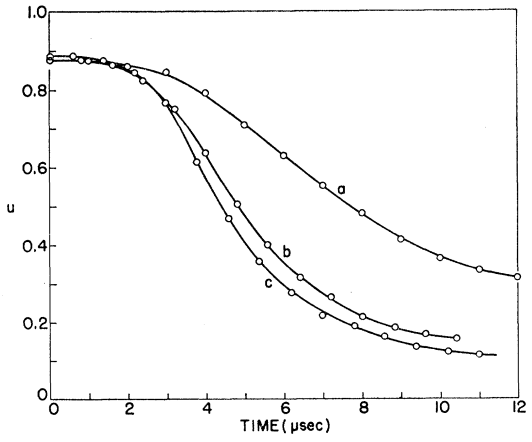

FIG. 5. Effect of ambient temperature on fast decay mode. Run 25. (a) 2.14°K; (b) 1.66°K; (c) 1.39°K.

[16] P. L. Scott, H. J. Stapleton, and C. Wainstein, Phys. Rev. **137**, A71 (1965).

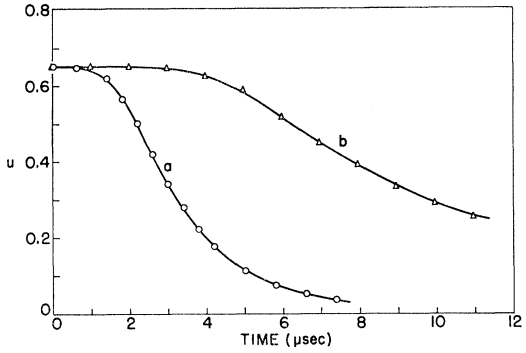

FIG. 6. Effect of thickness L on fast decay mode. $T=1.39$°K. (a) Run 21, $L=3$ mm, (b) run 25, $L=1.3$ mm. No great surface deterioration was observed between these measurements.

Crystals of dimensions roughly 5 mm×3 cm×3 cm were grown by slow evaporation from saturated aqueous solution at 0°C. They were relatively clear and free from imperfections. They were cut for mounting in the cavity into rectangular platelets typically 6×5×2 mm, with the minimum dimension perpendicular to the c axis. The samples were kept in sealed vials when not in use, in order to prevent the absorption of water. Storage in vacuum was found to be unsatisfactory, because the surfaces became powdery through loss of water.

V. RESULTS AND INTERPRETATION

In this section we present the experimental results and their interpretation. The time decay of the center of the line is described first, after which a discussion of the line shape is given.

In general, the decay profiles were found to depend on environmental temperature, initial spin temperature, size of the specimen, concentration of paramagnetic ion, and various historical details that presumably affected the surfaces of the crystals. As an aid in interpretation, some of the characteristics of the samples are summarized in Table I. Figures 5–8 illustrate the influence of temperature, initial conditions, surface, and size on the fast decay at negative spin temperature. All of these decay curves were measured by the method of Fig. 4(a).

In Fig. 5 are shown curves taken at three different temperatures on one sample, with approximately the same initial conditions. It is clear that the decay step is sharper at low temperature, where the indirect relaxation rate is small. At the highest temperature, 2.14°K, the indirect rates are comparable in magnitude to the direct rate,[11] but for the lower temperatures these rates are negligible. The small difference between 1.66 and

TABLE I. Characteristics of experimental runs and samples employed in study of spin-lattice relaxation in dilute cerous magnesium nitrate.

Experimental run	Frequency (GHz)	Nominal concentration (%)	Sample size (mm^3)	Remarks
12	11.12	0.5	6.5×6.5×2	New sample.
13	11.16	0.5	6.5×6.5×1	Same sample as run 12, but thinned in size.
15	11.14	0.2	8×6×2	New sample.
16	11.14	0.2	8×6×2	Same sample as run 15.
17	11.15	0.2	8×6×2	Same sample as runs 15 and 16. Sample maintained under vacuum at room temperature for several days prior to run; appeared dehydrated at end of experiment.
18	11.07	0.2	8×4×3	Sample obtained from same parent crystal as that of runs 15, 16, and 17.
21	11.12	0.2	7.5×5×3	New sample.
23	11.12	0.2	7.5×5×1.3	Same sample as run 21, but thinned in size.
24	11.20	0.2	7.5×5×1.3	Same sample as run 23, but experiment conducted more than a month later in time.
25	11.13	0.2	7.5×5×1.3	Same sample as run 24.
26	10.86	0.2(?)	8×6×3	New sample. Magnetic measurements indicate concentration $\gg 0.2\%$.
27	10.85	0.2(?)	8×6×3	Same sample as run 26.
28	11.21	0.2(?)	8×6×1	Same sample as runs 26 and 27, but thinned in size.

1.39°K is probably due to the fact that more energy is initially stored in the spin system, and less in the phonons, at the lower temperature; that is, the value of S becomes larger as the temperature is lowered.

The effect of sample size is shown in Fig. 6 which indicates that the avalanche is less severe with the thinner sample and/or after the sample has "aged" for a time (see Table I). It should be pointed out that it was impossible to separate completely the effects of sample size and age. Obviously, the sample could not be thinned without removing it from the spectrometer and therefore subjecting it to at least one thermal cycle. No obvious changes in surface texture had occurred between the two curves of Fig. 6. By way of

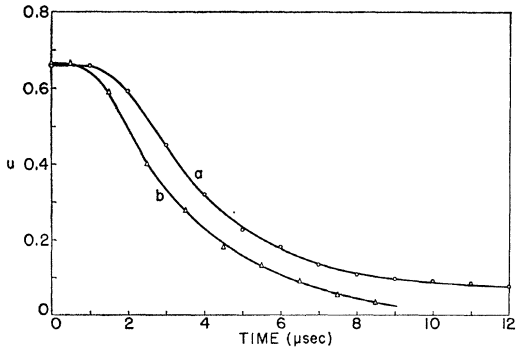

FIG. 7. Effect of surface condition on fast decay mode. (a) Run 17, after surface became powdery; (b) run 16, before. The difference is greatest near the end of the fast decay, where inversion persists much longer for (a). $T=1.37$°K.

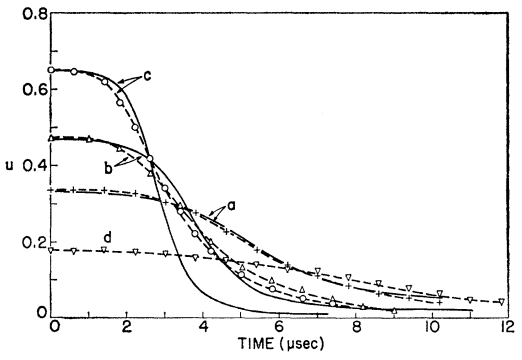

FIG. 8. Effect of initial spin temperature on fast decay mode. Run 21, $T=1.39$°K, $T_{1D}=7.75$ msec, $T_{1I}\rightarrow\infty$. Dashed lines connect experimental points; solid lines are solutions to Eqs. (1) for cases (a), (b), and (c), using $S=4\times10^4$, $T_p=\frac{4}{3}$ μsec as determined by fitting case (a). Theoretical curves have been shifted empirically to allow for initial phonon excitation and uncertainty in starting time: (a), $u(t-1.75)$; (b) $u(t-0.94)$; (c) $u(t-0.55)$. Fitting (c) instead of (a) gives $S=3\times10^4$, $T_p=1$ μsec; but the fit to (b) and (a) becomes much worse and larger time shifts are necessitated.

contrast, Fig. 7 compares the behavior of a sample on two successive data runs, between which the sample had been kept in vacuum at room temperature for several days. The surface had become visibly powdery and opaque. This deterioration was later found to be much less serious when samples were stored in sealed vials at room temperature, as was done for the case of Fig. 6.

Concentration was observed to have enormous influence on the fast decay profiles. No attempt was made to obtain quantitative measurements because of the unreliability of our concentration figures; however, it was invariably found that samples displaying stronger EPR absorption per unit volume showed stronger avalanche decays. (No concentration dependence, incidentally, was found for the direct or Raman relaxation rates measured on the same samples; the Orbach rates are discussed below.)

The easiest parameter to vary was the initial spin temperature, which could be altered simply by adjusting the amount of microwave power in the fast passage pulse. The data points and dashed lines of Fig. 8 show a typical family of decay curves obtained in this way. Since one parameter could be varied without affecting any of the others, these data were considered the most useful for a test of Eqs. (1). The results were less than reassuring. As is evident in Fig. 8, the model contains the general features of the decay curves but is totally incapable of quantitative prediction. If one adjusts S and T_p for a fit at the largest u^i, the curves for smaller u^i deviate markedly in the direction of increasing S and/or T_p with decreasing u^i. Conversely, if S and T_p are chosen for a fit at low u^i, they are far too large to accommodate the decay curves at higher initial spin temperatures.

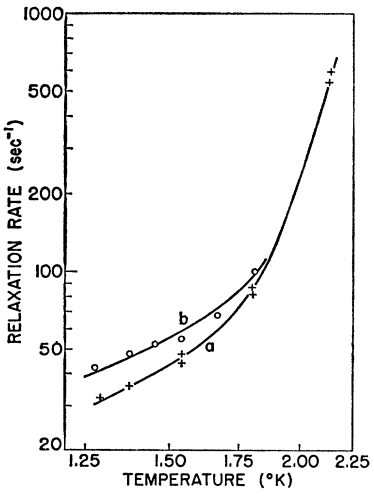

FIG. 9. Asymptotic decay rate versus temperature: effect of surface condition. (a) Runs 15 and 16, $\sigma=3.81/T$; (b) run 17, $\sigma=2.53/T$, same sample after storage in vacuum, resulting in pronounced surface deterioration. Smooth curves are Eq. (2). Compare with Fig. 7.

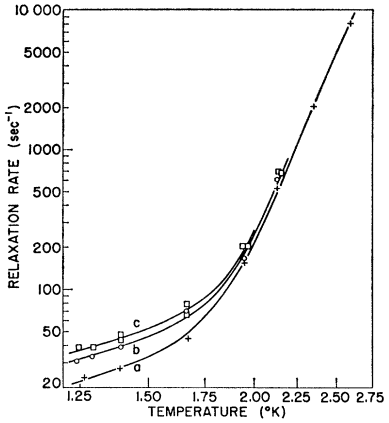

FIG. 10. Asymptotic decay rate versus temperature: influence of size. (a) Run 21, $L=3$ mm, $\sigma=5.58/T$; (b) run 23, $L=1.3$ mm, $\sigma=3.37/T$; (c) runs 24 and 25, one month after (b), $L=1.3$ mm, $\sigma=2.78/T$. The change in thickness has a much greater effect than the slow deterioration of the surface when the sample has been stored properly. Smooth curves are Eq. (2). Compare with Fig. 6.

Although one might expect a large acoustical mismatch at the crystal-helium interface, the data could only be fitted with phonon lifetimes corresponding closely to a matched boundary. This result is not unique to the present work; it has also been observed in numerous other hydrated paramagnetic salts.[4–6] Mills[17] has suggested that the surfaces of hydrated crystals may be nonreflecting in liquid helium; other possibilities include elastic scattering of the heated phonons into modes which interact only weakly with the ions, or inelastic scattering into modes which are not resonant and do not interact with the ions.

In all these curves, the starting time was treated as a third adjustable parameter. The time experimentally called zero was established by noting the time at which the absorption line reached its maximum (with field sweep but without pulse) and could have been in error by as much as one μsec; however, the theoretical curves had to be shifted toward earlier times by amounts up to two μsec in order to effect a best compromise with the experimental points. The time shift can be justified by assuming that some excitation is present in the phonon spectrum at the experimental $t=0$; however, the discrepancy between the theoretical and experimental shapes of the decay profiles is less easily explained. Some possible reasons will be discussed below.

At long times, near thermal equilibrium, the decay curves become exponential. The variation of the asymptotic rate T_{1A}^{-1} of Eq. (2) with temperature is shown in Figs. 9–10. Some of the points represent data from the same decay curves whose short time development is shown in Figs. 5–8; for others, the fast decay mode was not measured. In general, we found it useless to attempt quantitative interpretation of the comparative

[17] D. L. Mills, Phys. Rev. 133, A876 (1964).

decay curves for different samples, because the asymptotic time constants depended sensitively on the (unknown) concentration. For a given sample, however, it was perfectly straightforward to measure the variation of T_{1A} with temperature, thickness, and surface condition (although the last two parameters could not be properly separated from one another). According to the model, the time constant should have the temperature dependence of Eq. (2); and the bottleneck parameter $\sigma=B/DT$ should increase with increasing thickness and (presumably) decrease with increasing surface roughness.

Crude evidence for the dependence on surface finish is shown in Fig. 9. No statistically significant change in T_{1A} occurred between data runs 15 and 16, which occurred two days apart; but the bottleneck was clearly reduced during the four-day interval between 16 and 17, in which the sample was allowed to warm to room temperature under continuous pumping. As discussed earlier and shown in Fig. 7, the short time decay was also altered, and the surface was clearly damaged, by this treatment. In this connection, it was invariably found that the bottleneck diminished gradually with age for any given sample, but, as mentioned above, the aging could be retarded by storage under favorable conditions.

In Fig. 10 is shown an attempt to obtain, as nearly as possible, a "pure" size dependence. Ten days elapsed between 21 and 23 (run 22 was abortive), during which the sample was thinned and stored at room temperature in a sealed vial. No gross change in surface was apparent visually. A modest but real change in σ clearly occurred. Subsequent storage for a month under the same conditions, with no change in size, caused a change in σ which was much smaller. We therefore conclude that the primary effect was due to a change in size. Fast decay profiles for the same conditions are shown in Fig. 6, and they are consistent with the long-time behavior.

The smooth curves of Figs. 9–10 represent least-squares fits to the function

$$T_{1A}^{-1}=(1/6.02\times10^{-39}\nu^4T+1/DT^2)^{-1}$$
$$+0.09T^9+E\exp(-36.7/T)\ \text{sec}^{-1},$$

in which D and E were allowed to vary and the other parameters were taken from Ref. 11. The fits are satisfactory but by no means definitive. Other polynomial functions of $1/T$ would doubtless describe the direct component of the asymptotic rate equally well. It is interesting but perhaps fortuitous that the values of σ found from the asymptotic decays agree relatively well with the values which best describe the fast decays, even though the significance of the latter is rather dubious.

The Orbach coefficient E was not held constant in order to allow for the possibility of a bottleneck at the Orbach frequency.[11] For various concentrations, sizes, and surface conditions, such a bottleneck might appear as a correlation between σ and E. In Table II we give these two parameters for all data runs in which T_{1A} was measured. The sample for 26–28 was much more concentrated than its predecessors, as evidenced by the magnitude of its spin resonance line; in fact, the avalanche was too fast to observe, and only the asymptotic decay rates were measured. It appears that the Orbach coefficient varies moderately with concentration, but the dependence on other parameters is weaker or nonexistent.

In summary, the asymptotic decay mode exhibits a variation with temperature, thickness of sample, and concentration (to the extent it was measured) in keeping with the model based on simple rate equations, while the fast decay mode agrees only in a qualitative sense and disagrees in the details of the shape of the decay profiles and the dependence on initial spin temperature. The model contains so many questionable assumptions that it is difficult to isolate the ones at fault. One possibility involves the constancy of the parameter S. This quantity contains a linewidth which is rather loosely defined as a measure of the energy width of the lattice modes capable of direct interaction with the ions. If this linewidth should be time-dependent, the decay profiles would of course be altered. In particular, if the interaction width broadened during the decay, the experimental curves would deviate in just the observed direction (decreasing S with increasing time).

For this reason, the variation with time of the shape of the spin resonance line was observed by means of the technique of Fig. 4(b). In Fig. 11 are shown photographs of the line taken at various stages during the decay. This sequence was obtained on a newly prepared sample for which the temperature variation of the asymptotic decay yielded $\sigma=4.7/T$. The temperature was relatively high so that the bottleneck was modest. The zero of time is arbitrary and corresponds to a soaking interval of zero. Immediately after inversion, the line shape was normal. As time continued, however, the center recovered faster than the wings, giving birth

TABLE II. Values of Orbach coefficient E and bottleneck factor σ for asymptotic time constant T_{1A} of dilute cerous magnesium nitrate crystals.

Experimental run	$E\times10^{-10}$ (sec^{-1})	σ
12	1.03	$4.52/T$
13	1.03	$3.29/T$
15, 16	1.14	$3.81/T$
17	1.14	$2.53/T$
18	1.14	$4.71/T$
21	1.08	$5.58/T$
23	1.14	$3.37/T$
24, 25	1.14	$2.78/T$
26, 27	0.79	$18.0/T$
28	0.79	$11.5/T$

to a hole in the line; and the normal line shape was regained only long after the avalanche in the center had terminated. Thereafter the shape remained normal. This hole was never observed in decays measured at lower frequencies,[11] where the bottleneck is absent, and is apparently a direct consequence of the avalanche.

In order to provide added insight, a sequence similar to Fig. 11 was recorded but the initial spin temperature was deliberately made nonuniform. Figure 12 shows tracings made from photographs taken during the same data run (18) at a lower temperature, where the bottleneck was somewhat stronger. Three initial conditions are shown: no inversion, inversion of the full line, and inversion of one half of the line. Comparison of the last two indicates that no significant diffusion of energy occurs during the time the central portions of the line undergo an avalanche, although a small amount might be present.[18]

The point to be stressed is that the spin resonance line appears to be essentially inhomogeneous on the time scale of an avalanche but homogeneous for times somewhat shorter than that of the asymptotic decay. The line must still be inhomogeneous at times for which the spin temperature changes sign, typically 500 μsec; otherwise the direct-rate data of Ref. 11 would have been distorted and the dependences $T_{1D}^{-1} \propto H^4 T$ would not have been found. (Recall that these measurements were taken from slopes at $u=0$.) Spectral diffusion must be present over long times, because the spin temperature becomes and remains uniform throughout the line after several milliseconds. If there were no homogenizing mechanism, the line shape would have to be abnormal at long times, because spin packets in the wings would be less severely bottlenecked than those in the center and so would recover faster. The line would appear to become blunted.

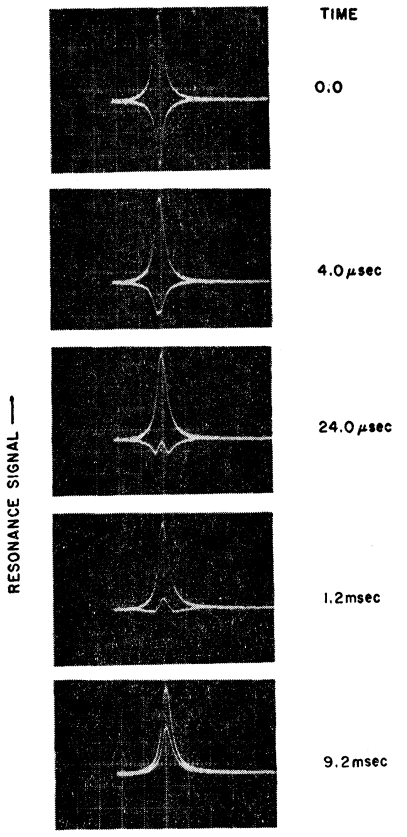

FIG. 11. Appearance of line at various times during recovery. Reference traces of normal absorption line are also shown. Run 18 at 1.67°K. Zero of time corresponds to first measurement, not to fast passage.

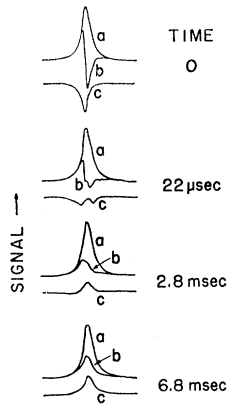

FIG. 12. Appearance of line at various times during recovery. (a) Normal absorption line, (b) after fast passage of half of the line, (c) after fast passage of entire line. Run 18 at 1.24°K.

These results are consistent with at least two explanations. On one hand, the quantity $d\nu$ in Eqs. (1) might increase with time by virtue of the nonlinear spin-phonon interaction itself. The broadening could be too small to lie within the resolution of our apparatus but large enough to accommodate the differences between theoretical and observed fast decay profiles for the line center. In this connection, it may be significant that the inverse phonon lifetime, the width of a spin packet (as obtained from spin-echo data[19]), and the interruption rate for a phonon, $A(n_2-n_1)/\rho(\nu)d\nu$, are all of the same order, so that the spin-phonon interaction is indeed very strong. During the decay the interruption rate changes in magnitude and the effect might well appear as a time varying interaction width. Unfortunately, no adequate theory exists at present.

A second possibility involves the phonon lifetime rather than the linewidth. If the phonon excitation should become large enough during the fast decay to be damped by nonlinear phonon-phonon interactions, the fast decay would be affected in the manner observed.

Over long times, some mechanism of spectral diffusion not involving the ion-phonon interaction would appear to be necessary in order to render the line homogeneous on the time scale of the conventional

[18] The small asymmetry apparent in tracing c at 22 μsec is thought to be incidental. This skewing was always present at the lowest temperatures and probably occurred because the part of the line observed last had been swept through the band of hot phonons generated in the avalanche of the line center.

[19] J. A. Cowen and D. E. Kaplan, Phys. Rev. **124**, 1098 (1961).

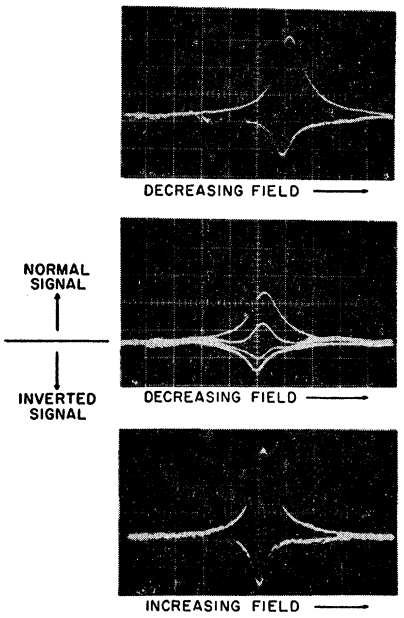

FIG. 13. Inverted line superimposed on normal line for various samples, showing shift of resonant field with spin temperature at high concentration. Upper photo: run 26, $T=2.16$°K, dimensions $8\times6\times3$ mm³. Center: also run 26, but $T=1.96$°K. Lower photo: run 28, $T=1.95$°K. Same sample after thinning to $8\times6\times1$ mm³ shows a field shift of opposite sign. Time base is 2 μsec/major division for all cases.

phonon bottleneck. Spin-spin coupling, for example, could easily suffice.

VI. SUMMARY

The anomalous decay from an initial state of negative spin temperature to the environmental temperature behaves in full qualitative accord with a model based on the hypothesis that the resonant lattice modes interact more strongly with the paramagnetic ions than with the thermal bath. Fast and slow decay modes, corresponding to negative and positive spin temperature, depend sensitively on the size of the specimen, its surface, the initial spin temperature, the bath temperature, the Zeeman field, and the concentration of paramagnetic ions. The over-all evidence is so overwhelming and the behavior so unique as to rule out any model not involving a phonon bottleneck.[20]

Quantitative discrepancies, however, do exist between experiment and theory; they undoubtedly stem from the naivete of the model. An excitation-dependent phonon lifetime and/or linewidth for the interaction are proposed as possible explanations, but further work will be required to distinguish them. Finally, there is considerable evidence for spin diffusion on a time scale intermediate between the fast and slow decay modes.

[20] N. S. Shiren [Phys. Rev. Letters **17**, 958 (1966)] has recently reported the direct detection of avalanche phonons in MgO doped with divalent iron. This work appears to provide final confirmation of the avalanche mechanism.

ACKNOWLEDGMENTS

The authors wish to thank W. B. Mims for his continued encouragement and valuable suggestions. We are indebted to J. M. Minkowski for his helpful advice, to Z. H. Schroeder for the construction of the cavity, and to J. W. Leight for the preparation of the crystals.

APPENDIX

The photos of Fig. 13 depict cases in which the resonant field for the inverted spin resonance line has been shifted to both lower and higher values relative to the field of the thermalized resonance line. If one attempts to monitor continuously the relaxation of the line center after an initial perturbation, this line shift, which itself changes with time, will distort the data.

The effect has a simple classical explanation. For a paramagnetic sample obeying the Curie law, the applied magnetic field for resonance is

$$H_0=(h\nu/g\beta)[1-(\tfrac{4}{3}\pi-N)(C/T)],$$

where ν is the microwave oscillator frequency, T is the absolute temperature characterizing the spin system, C is the Curie constant for the material, and N is the demagnetization factor determined by the sample shape. (C is proportional to the density of paramagnetic ions; for a rectangular platelet, N varies from 0 to 4π as the sample dimension parallel to the applied magnetic field goes from a very large value to a very small one.) The last term in the above expression represents the effect of spin magnetization on the local field in the sample and, at liquid-helium temperatures, becomes significant in determining the resonant-field value for the thermalized resonance line. Then, when the spin system is perturbed into a negative temperature state, the resonant field for the inverted line is displaced relative to that for the equilibrium resonance; and, as the spin system decays back toward equilibrium, the resonant field also returns gradually to its thermalized value.

For dilute cerous magnesium nitrate, an ion concentration of 0.2% yields $C\sim2\times10^{-5}$°K. If one assumes a bath temperature of 1°K and $(4\pi/3-N)\sim5$, a total inversion of the resonance line causes a field shift of 0.02%; at 11 GHz and a resonant field of 4400 G, this change is 0.9 G. Since the total linewidth is typically 5 G, the shift will be quite pronounced and may, in many instances, invalidate the continuous method of data collection.

For a large sample of high concentration, the upper photo of Fig. 13 shows the inverted line shifted to a higher resonant field than that of the thermalized line. The center photo shows this same sample at different spin temperatures; the varying resonant field is unmistakable. The field shift for this sample after its characteristic length has been decreased by a factor of three is depicted in the last photo. The inverted resonance line is now displaced to a lower field because of a change in sign of $(4\pi/3-N)$ with an increase in N.

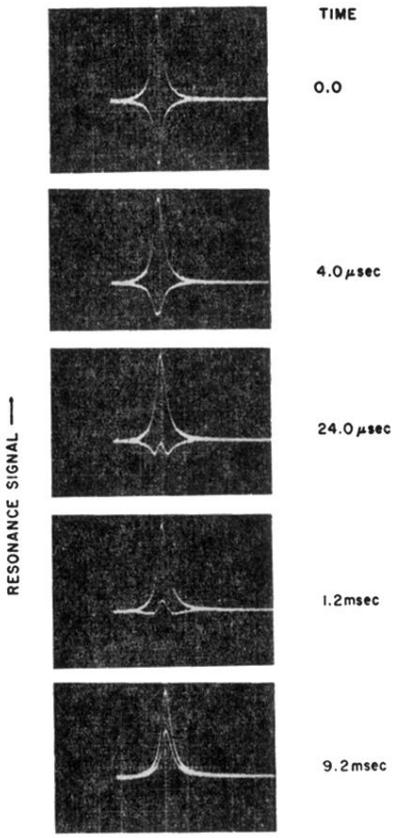

FIG. 11. Appearance of line at various times during recovery. Reference traces of normal absorption line are also shown. Run 18 at 1.67°K. Zero of time corresponds to first measurement, not to fast passage.

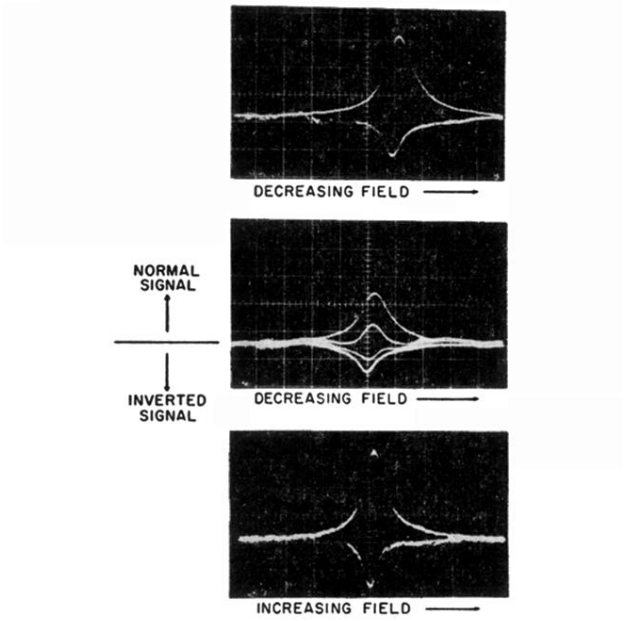

FIG. 13. Inverted line superimposed on normal line for various samples, showing shift of resonant field with spin temperature at high concentration. Upper photo: run 26, $T=2.16°K$, dimensions $8\times6\times3$ mm^3. Center: also run 26, but $T=1.96°K$. Lower photo: run 28, $T=1.95°K$. Same sample after thinning to $8\times6\times1$ mm^3 shows a field shift of opposite sign. Time base is 2 μsec/major division for all cases.